

Insulin Granule Recruitment and Exocytosis Is Dependent on p110 γ in Insulinoma and Human β -Cells

Gary M. Pigeau,¹ Jelena Kolic,¹ Brandon J. Ball,¹ Michael B. Hoppa,² Ying W. Wang,¹ Thomas Ruckle,³ Minna Woo,⁴ Jocelyn E. Manning Fox,¹ and Patrick E. MacDonald¹

OBJECTIVE—Phosphatidylinositol 3-OH kinase (PI3K) has a long-recognized role in β -cell mass regulation and gene transcription and is implicated in the modulation of insulin secretion. The role of nontyrosine kinase receptor-activated PI3K isoforms is largely unexplored. We therefore investigated the role of the G-protein-coupled PI3K γ and its catalytic subunit p110 γ in the regulation of insulin granule recruitment and exocytosis.

RESEARCH DESIGN AND METHODS—The expression of p110 γ was knocked down by small-interfering RNA, and p110 γ activity was selectively inhibited with AS605240 (40 nmol/l). Exocytosis and granule recruitment was monitored by islet perfusion, whole-cell capacitance, total internal reflection fluorescence microscopy, and electron microscopy in INS-1 and human β -cells. Cortical F-actin was examined in INS-1 cells and human islets and in mouse β -cells lacking the phosphatase and tensin homolog (PTEN).

RESULTS—Knockdown or inhibition of p110 γ markedly blunted depolarization-induced insulin secretion and exocytosis and ablated the exocytotic response to direct Ca²⁺ infusion. This resulted from reduced granule localization to the plasma membrane and was associated with increased cortical F-actin. Inhibition of p110 γ had no effect on F-actin in β -cells lacking PTEN. Finally, the effect of p110 γ inhibition on granule localization and exocytosis could be rapidly reversed by agents that promote actin depolymerization.

CONCLUSIONS—The G-protein-coupled PI3K γ is an important determinant of secretory granule trafficking to the plasma membrane, at least in part through the negative regulation of cortical F-actin. Thus, p110 γ activity plays an important role in maintaining a membrane-docked, readily releasable pool of secretory granules in insulinoma and human β -cells. *Diabetes* 58: 2084–2092, 2009

From the ¹Department of Pharmacology and the Alberta Diabetes Institute, University of Alberta, Edmonton, Alberta, Canada; the ²Oxford Centre for Diabetes, Endocrinology and Metabolism, University of Oxford, Headington, Oxford, U.K.; ³Geneva Research Center, Merck Serono, Geneva, Switzerland; and the ⁴Department of Medicine, Medical Biophysics, Institute of Medical Science, Ontario Cancer Institute, University of Toronto, Toronto, Ontario, Canada.

Corresponding author: Patrick E. MacDonald, pmacdonald@pmcol.ualberta.ca.

Received 6 October 2008 and accepted 3 June 2009.

Published ahead of print at <http://diabetes.diabetesjournals.org> on 23 June 2009. DOI: 10.2337/db08-1371.

G.M.P. and J.K. contributed equally to this article.

© 2009 by the American Diabetes Association. Readers may use this article as long as the work is properly cited, the use is educational and not for profit, and the work is not altered. See <http://creativecommons.org/licenses/by-nc-nd/3.0/> for details.

The costs of publication of this article were defrayed in part by the payment of page charges. This article must therefore be hereby marked "advertisement" in accordance with 18 U.S.C. Section 1734 solely to indicate this fact.

Phosphatidylinositol 3-OH kinase (PI3K) signaling has well-defined roles in the regulation of islet gene transcription and mass; however, its function in regulating glucose-stimulated insulin secretion remains a matter of debate. The use of nonselective pharmacological inhibitors has suggested both negative (1–3) and positive (4,5) roles for PI3K in insulin secretion. While a negative role is supported by the enhanced secretion seen following genetic downregulation of PI3K (3), a positive role is indicated by reduced insulin secretion following knockout of the insulin or IGF-1 receptor (6,7) or insulin receptor substrate-1 (8). In line with these observations, secretion is enhanced following β -cell-specific ablation of the phosphatase and tensin homolog (PTEN), which antagonizes PI3K signaling (9).

Type I PI3Ks catalyze the phosphorylation of PtdIns(4,5)P₂ to generate PtdIns(3,4,5)P₃ (10). Receptor tyrosine kinase-linked PI3Ks, which include the type 1A catalytic subunits (p110 α , - β , and - δ), modulate ion channel activity, Ca²⁺ signaling, and exocytosis (11–13). The lone type 1B PI3K, containing the p110 γ catalytic subunit, is activated by G-protein-coupled receptors (14), exhibits basal lipid kinase activity (15), and regulates cardiac contractility and inflammation (16). Activity of p110 γ has been detected in insulinoma cells, where it is activated by glucose-dependent insulinotropic polypeptide (GIP) (17). Furthermore, we have demonstrated expression of this isoform in mouse and human islets (18) and a lack of first-phase insulin secretion in p110 γ knockout mice (18,19).

We have now examined the mechanism by which p110 γ regulates insulin exocytosis in INS-1 and mouse and human β -cells. We find that this PI3K isoform regulates β -cell Ca²⁺-dependent exocytosis by controlling the size of the membrane-associated pool of secretory granules. Furthermore, we identify a role for p110 γ in the modulation of cortical F-actin density as a mechanism by which it can regulate access of secretory granules to the plasma membrane. Thus, we now show that p110 γ plays an important role in maintaining the ability of β -cells to undergo a robust secretory response following stimulation.

RESEARCH DESIGN AND METHODS

Cells and cell culture. INS-1 832/13 and 833/15 cells (20,21) (from Prof. C. Newgard; Duke University) were transfected with Lipofectamine 2000 (Invitrogen, Carlsbad, CA), according to supplier instructions, and replated on glass coverslips for total internal reflection fluorescence (TIRF) or 35-mm culture dishes for patch clamp.

Islets from RIP-cre⁺/PTEN^{+/+} and RIP-cre⁺/PTEN^{fl/fl} mice (9) and from wild-type C57/bl6 mice were isolated by collagenase digestion followed by hand picking. Human islets from 13 healthy donors were from the Clinical Islet Laboratory at the University of Alberta. All studies were approved by the animal care and use committee and the human research ethics board, as

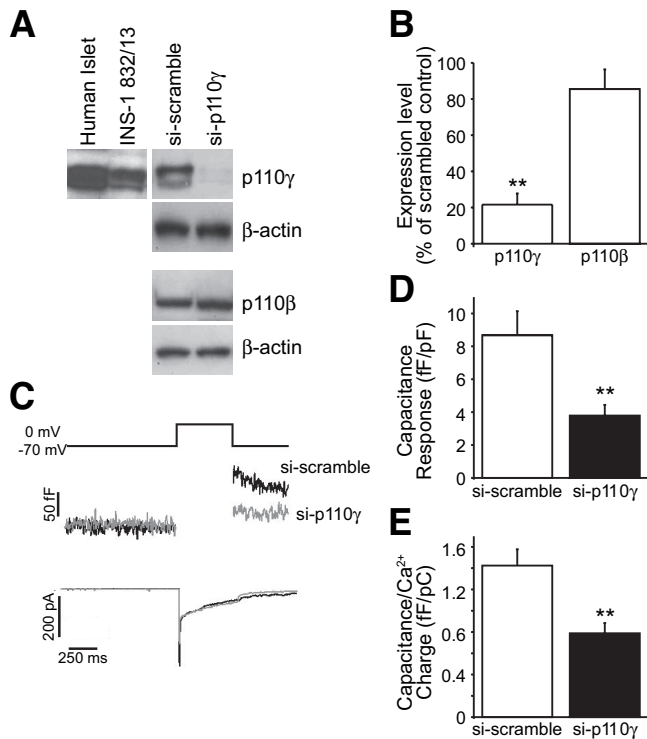


FIG. 1. Expression of p110 γ and effect of siRNA knockdown. **A:** Expression of p110 γ was confirmed by Western blot of protein lysates from human islets and INS-1 832/13 cells (*left*). Expression of p110 γ , but not the related p110 β , was reduced by an adenovirus-delivered si-p110 γ construct in INS-1 832/13 cells (*right*). **B:** The average expression levels of p110 γ and p110 β in the si-p110 γ INS-1 832/13 cells is shown normalized to β -actin and expressed as a percentage of the si-scramble control. **C:** Capacitance and Ca²⁺ current recordings from INS-1 832/13 cells expressing si-scramble (black lines) or si-p110 γ (gray lines). **D and E:** The average capacitance response is shown, normalized to cell size (**D**) and Ca²⁺ current charge (**E**). ** $P < 0.01$.

appropriate, at the University of Alberta. Islets were dispersed to single cells by incubation for 11 min at 37°C in Ca²⁺-free dispersion buffer followed by gentle trituration with a flame-polished glass pipette. Mouse islets and cells were cultured in RPMI media with L-glutamine and supplemented with 10% fetal bovine serum (FBS) and 100 units/ml penicillin/streptomycin. Human islets and cells were cultured in low-glucose (1g/l) DMEM with L-glutamine, 110 mg/l sodium pyruvate, and supplemented with 10% FBS and 100 units/ml penicillin/streptomycin.

Islet perfusion was performed using a Brandel SF-06 system (Gaithersburg, MD) following 2 h static preincubation in 5 mmol/l KCl Krebs-Ringer bicarbonate (KRB) (in mmol/l: NaCl 115; KCl 5; NaHCO₃ 24; CaCl₂ 2.5; MgCl₂ 1; HEPES 10; 0.1% BSA, pH7.4; and 40 nmol/l AS605240 or DMSO alone). Seventy-five human islets per lane were perfused at 0.25 ml/min. Solutions were switched to 50 mmol/l KCl KRB (50 mmol/l KCl replaced an equivalent amount of NaCl) as indicated. Perifusate was stored at -20°C and analyzed for insulin via enzyme-linked immunosorbent assay (Alpco, Salem, NH).

DNA and adenovirus constructs. The p110 γ siRNA has been published previously (19). A scrambled control sequence (GCTAAATAATCGGATGATGT) was generated using Genscript (Piscataway, NJ) small-interfering RNA (siRNA) target finder software, synthesized as a hairpin oligo with *Bam*HI and *Hind*III restriction sites on the 5' and 3' ends, respectively, and ligated into the pRNAT-H1.1/shuttle vector (Clontech, Mountain View, CA). For most experiments, these were transfected into INS-1 832/13 or human β -cells by lipid transfection (Lipofectamine 2000), followed by 72 h of culture. For some experiments (Fig. 1A and B), expression was via recombinant adenovirus produced by transferring the expression cassettes into the Adeno-X viral vector (Clontech) followed by adenovirus production in HEK293 cells. HEK293 cell lysates were used to infect INS-1 832/13 cells for 5 h at a concentration previously determined for maximum infection efficiency. Cells were then washed and cultured for an additional 72 h.

The VAMP-pHlourin construct was from Prof. G. Miesenboeck (University of Oxford). The NPY-mCherry and islet amyloid polypeptide (IAPP)-mCherry were created by ligating the mCherry sequence (Prof. R. Tsien, University of

California San Diego, CA) in place of the RFP of an NPY-RFP construct (Prof. G. Rutter, Imperial College London, London, U.K.) or the emerald of an IAPP-emerald construct (22).

Pharmacologic inhibition of p110 γ . 5-Quinoxilin-6-methylene-1,3-thiazolidine-2,4-dione (AS605240; Merck Serono, Geneva, Switzerland) is an ATP-competitive inhibitor of p110 γ ($K_i = 8$ nmol/l). Culture media was supplemented with 40 nmol/l AS605240 in DMSO or an equal volume of DMSO alone. This compound selectively targets p110 γ ($K_i = 60$ nmol/l, 270 nmol/l, and 300 nmol/l for p110 α , - β , and - δ , respectively) and exhibits no notable activity against a wide array of protein kinases at 1 μ mol/l (23). Consistent with a lack of effect on the type 1A PI3Ks, treatment of INS-1 832/13 cells overnight with 40 nmol/l AS605240 did not block PI3K activation in response to high K⁺, which activates type 1A PI3K through an autocrine insulin effect (24). This was assessed by recruitment of the green fluorescent protein-tagged PH domain of the general receptor for phosphoinositides (GFP-GRP1_{PH}) (25), where 25 mmol/l KCl elicited a 2.7 \pm 0.4-fold increase in DMSO-treated cells ($n = 11$) and a 2.9 \pm 0.2-fold increase in AS605240-treated cells ($n = 9$).

Immunoblotting. Lysates were subjected to SDS-PAGE and transferred to polyvinylidene difluoride membranes (Millipore, Billerica, MA), probed with primary antibodies (anti-p110 γ , anti-p110 β , and anti- β -actin; Santa Cruz Biotechnology, Santa Cruz, CA), detected with peroxidase-conjugated secondary anti-mouse or anti-rabbit antibodies (Santa Cruz Biotechnology), and visualized by chemiluminescence (ECL-Plus; GE Healthcare, Mississauga, Canada) and exposure to X-ray film (Fujifilm, Tokyo, Japan). Western blot analysis of F- and G-actin was performed using the G-actin/F-actin In Vivo Assay Kit (Cytoskeleton, Denver, CO). Densitometry was expressed relative to total actin.

Electrophysiology. We used the standard whole-cell technique with the sine+DC lockin function of an EPC10 amplifier and Patchmaster software (HEKA Electronics, Lambrecht/Pfalz, Germany). Experiments were performed at 32–35°C. Extracellular bath solution for depolarization trains contained (in mmol/l) 118 NaCl, 20 TEA, 5.6 KCl, 1.2 MgCl₂ · 6H₂O, 2.6 CaCl₂, 5 glucose, and 5 HEPES (pH 7.4 with NaOH). Pipette solution for depolarization trains contained (in mmol/l) 125 Cs-glutamate, 10 CsCl, 10 NaCl, 1 MgCl₂ · 6H₂O, 0.05 EGTA, 5 HEPES, and 3 MgATP (pH 7.15 with CsOH). The pipette solution also contained 0.1 mmol/l cAMP or 10 μ mol/l latrunculin, as indicated. For Ca²⁺ infusion experiments, the extracellular bath contained (in mmol/l) 138 NaCl, 5.6 KCl, 1.2 MgCl₂ · 6H₂O, 2.6 CaCl₂, 5 glucose, and 5 HEPES (pH 7.4 with NaOH). Pipette solution for Ca²⁺ infusion contained (in mmol/l) 125 K-glutamate, 10 NaCl, 10 KCl, 1 MgCl₂ · 6H₂O, 5 CaCl₂, 10 EGTA, 5 HEPES, and 3 MgATP (pH 7.1 with KOH) for 200 nmol/l free-Ca²⁺. Patch pipettes, pulled from borosilicate glass and coated with Sylgard, had resistances of 3–4 megaohm (Ω) when filled with pipette solution. Whole-cell capacitance responses were normalized to initial cell size and expressed as femtofarad per picofarad (fF/pF).

Microscopy. An Olympus IX71 inverted microscope with a PlanApo 100 \times objective (NA 1.45; Olympus Canada, Markham, Canada) was used for TIRF microscopy. Excitation was established with a 488-nm Argon laser and a 543-nm He-Ne laser (Melles Griot, Carlsbad, CA), passing through a laser combiner, a single-mode optical fiber with laser coupler (458–633 nm), and an IX2-RFAEVA-2 TIRFM illuminator (Olympus Canada). Emission was separated with a GFP/RFP dichroic (Chroma, Rockingham, VT), filtered with a GFP (520–535 nm) or RFP filter set (590–650 nm; Chroma), and projected onto a back-illuminated Rolera-Mgi Plus EMCCD camera (Q Imaging, Surrey, Canada) operated by InVivo version 3.2.0. (Media Cybernetics, Bethesda, MD). For TIRF/patch-clamp experiments, cells were imaged (16.7 Hz) with a Cascade II 512 EMCCD camera (Photometrics, Tucson, AZ), and cell capacitance was recorded as above. For visualization of actin, cells were fixed with Z-FIX (Anatech, Battle Creek, MI) and stained with Alexa Fluor 488-conjugated phalloidin (Invitrogen).

For epifluorescence microscopy, cells were fixed and stained for actin as above and positively identified as β -cells by immunostaining (rabbit anti-insulin primary antibody, donkey anti-rabbit IgG secondary antibody conjugated to Texas Red; Santa Cruz Biotechnology). Cells were imaged with an Olympus BX61 upright microscope and a 60 \times LumPlanF objective (0.9 NA). Excitation was with a DG4 light source with either a tetramethyl rhodamine isothiocyanate or fluorescein isothiocyanate filter set (Semrock, Rochester, NY). For clarity, only the green channel (F-actin staining) is shown (Fig. 6A). Images were captured with a Retiga Exi CCD camera (Q Imaging) operated by InVivo version 3.2.0 (Media Cybernetics).

For electron microscopy, cells were prefixed in 2.5% glutaraldehyde in cacodylate buffer solution (pH 7.3) for 1.5 h at room temperature then washed and post fixed with 1% osmium tetroxide in the same buffer for 1.5 h. Following a wash in distilled water, the sample was dehydrated in a graded series of ethanol solutions (50, 70, and 90% for 10 min each) before the final two additional 10 min with absolute ethanol. Samples were then embedded in

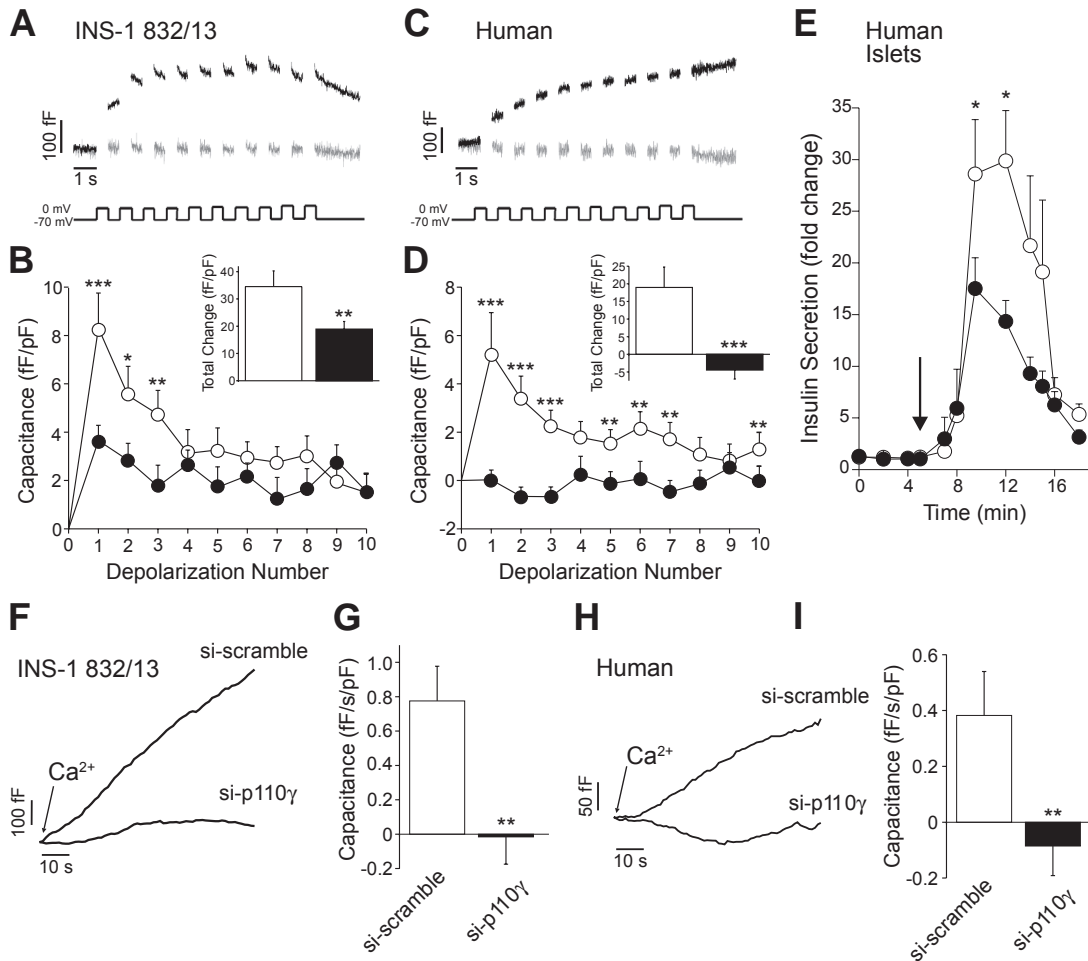


FIG. 2. Effect of p110 γ knockdown and inhibition on depolarization and Ca²⁺-evoked insulin exocytosis. **A:** Capacitance recordings are shown from INS-1 832/13 cells expressing si-p110 γ (gray lines) or si-scrambled (black lines). **B:** The average capacitance response during each depolarization for cells expressing si-p110 γ (●) or si-scrambled (○) and the total capacitance change over the depolarization train (*inset*). **C and D:** Show the same as **A** and **B**, except data are from human β -cells, identified by positive insulin immunostaining, treated overnight with DMSO (black lines, ○) or the p110 γ inhibitor AS605240 (40 nmol/l) (gray lines, ●). **E:** Insulin secretion was measured by perfusion of isolated human islets following overnight treatment with DMSO (○) or 40 nmol/l AS605240 (●). **F:** Exocytosis was stimulated in INS-1 832/13 cells expressing si-p110 γ or si-scrambled by direct infusion of 200 nmol/l free Ca²⁺ and observed as an increase in capacitance. **G:** The average rate of capacitance increase at steady state (30–60 s). **H and I:** Show the same as **E** and **F**, except data are from human β -cells expressing si-p110 γ or the si-scramble. * $P < 0.05$; ** $P < 0.01$; *** $P < 0.001$.

Spurr's resin and cured at 70°C for 10 h. Ultrathin sections were stained with 2% uranyl acetate for 30 min and lead citrate for 5 min. Micrographs were taken at 75 Kv with a Hitachi transmission electron microscope H-7000 (Tokyo, Japan). All imaging data were analyzed with either ImageJ 1.38 \times (National Institutes of Health) or Image Pro Plus version 6.2 (Media Cybernetics).

RESULTS

PI3K catalytic subunit expression and knockdown in insulin-secreting cells. Expression of p110 β and - γ was confirmed in INS-1 832/13 cells and human islets by Western blot (Fig. 1A) and RT-PCR (not shown), in agreement with previous reports (18,19,26). Expression of an siRNA construct targeted against p110 γ (si-p110 γ) (19) in INS-1 832/13 cells reduced p110 γ expression by 78% ($n = 3$) compared with a scrambled siRNA (si-scrambled) control (Fig. 1A and B). Expression of the type 1A p110 β isoform, which can functionally compensate for p110 γ (27), was not affected by the p110 γ siRNA (Fig. 1A and B). **PI3K γ regulates insulin exocytosis.** Whole-cell membrane capacitance changes and voltage-dependent Ca²⁺ channel activity were monitored in INS-1 832/13 cells

expressing si-p110 γ or si-scrambled (Fig. 1). The capacitance response to a 500-ms membrane depolarization was decreased by 56% ($P < 0.01$, $n = 20$ and 19) upon p110 γ knockdown (Fig. 1C and D). The Ca²⁺ current charge during this depolarization was not different between groups (-4.82 ± 0.64 and -6.62 ± 0.93 pC/pF; $n = 20$ and 18, NS). When normalized to Ca²⁺ charge, the exocytotic response was reduced 45% by knockdown of p110 γ ($P < 0.01$) (Fig. 1E).

We used membrane depolarization trains to further assess the effect of p110 γ knockdown on exocytosis. The total capacitance response was decreased by 45% upon expression of si-p110 γ ($n = 20$ and 18, $P < 0.05$) (Fig. 2A and B). Notably, the response to the first two depolarizations, considered to represent exocytosis of the readily releasable granule pool (28), was markedly blunted (by 54%, $P < 0.01$). A two-pulse analysis estimates a 60% reduction in readily releasable pool size from 22.4 ± 5.3 to 9.1 ± 1.3 fF/pF ($P < 0.05$).

Similarly, overnight inhibition of p110 γ with 40 nmol/l AS605240 ablated the exocytotic response of human

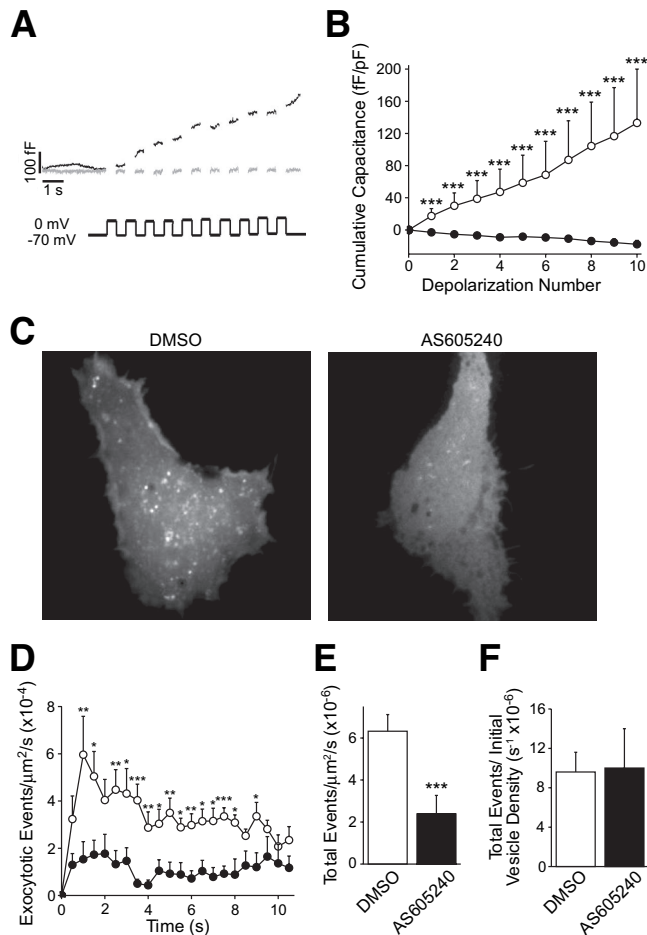


FIG. 3. Simultaneous TIRF microscopy and patch-clamp electrophysiology. INS-1 833/15 cells expressing a granule-targeted VAMP-pHluorin construct were simultaneously studied by whole-cell capacitance measurements and laser TIRF microscopy. **A:** Capacitance recordings during a train of membrane depolarizations are shown from INS-1 833/15 cells treated overnight with 40 nmol/l AS605240 (gray lines) or DMSO (black lines). **B:** The cumulative capacitance change over the depolarization train. **C:** Maximum-intensity projections over the course of the 10-s depolarization protocol, illustrating exocytotic release sites in DMSO- and AS605240-treated cells. **D:** The rate of exocytotic events visualized during depolarization trains over time applied to INS-1 833/15 treated overnight with DMSO (○) or 40 nmol/l AS605240 (●). **E:** The total rate of exocytotic events observed by TIRF over the depolarization train, and in **F** this is normalized to the initial granule number. *** $P < 0.001$.

β -cells identified by positive insulin immunostaining ($n = 18$ cells from five donors, $P < 0.001$) (Fig. 2C and D) without affecting Ca^{2+} currents (-0.61 ± 0.13 vs. -0.69 ± 0.19 pC/pF, $n = 15$ –18 cells from five donors). Consistent with an impairment of insulin granule exocytosis, per se, inhibition of p110 γ (40 nmol/l AS605240) in human islets resulted in a 51% reduction in peak insulin secretion to depolarization by 50 mmol/l KCl ($n = 11$ groups from four donors, $P < 0.05$) (Fig. 2E). Comparable results were also obtained from mouse islets (not shown).

Direct infusion of Ca^{2+} into the cell is often used as a measure of the Ca^{2+} -dependent recruitment of granules and their subsequent exocytosis (28). The capacitance response to infusion of 200 nmol/l free Ca^{2+} was blunted by expression of si-p110 γ in both INS-1 832/13 and human β -cells (Fig. 2F–D). Upon knockdown of p110 γ , the exocytotic response at 30–60 s was ablated in the INS-1 832/13 cells ($n = 8$, $P < 0.01$) and human β -cells ($n = 7$ cells from two donors, $P < 0.05$).

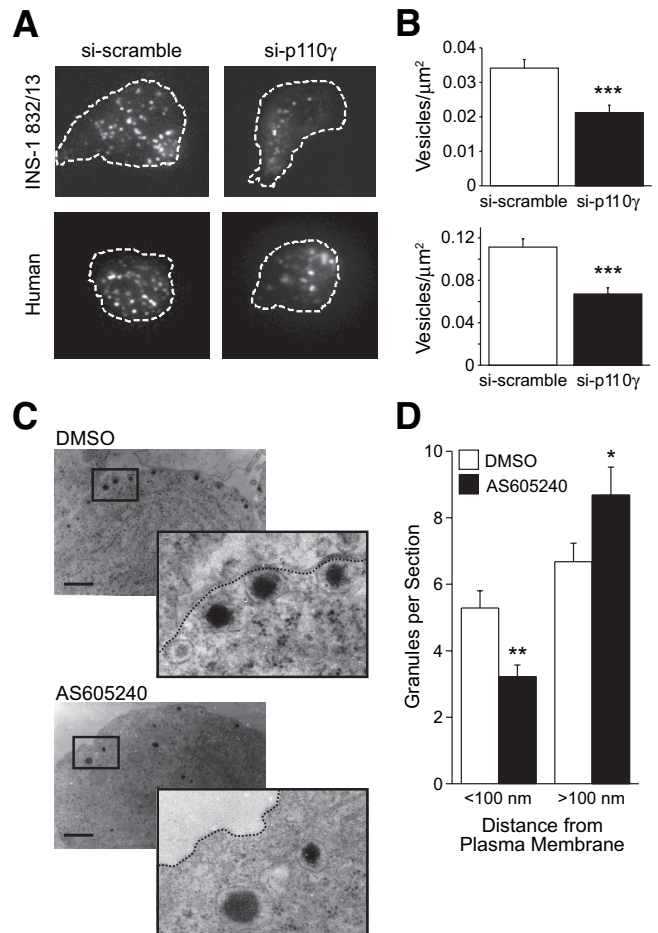


FIG. 4. Effect of p110 γ knockdown and inhibition on membrane localization of granules. **A:** Representative images of membrane-associated granules imaged by TIRF microscopy from INS-1 832/13 cells and human β -cells expressing either si-scramble or si-p110 γ together with the granule-targeted NPY-mCherry. **B:** The average membrane-associated granule density from the TIRF images, normalized to total membrane area. **C:** Electron micrographs were obtained from INS-1 832/13 cells under control conditions (DMSO) or following inhibition of p110 γ (40 nmol/l AS605240). **D:** The average number of granules per section located < and >100 nm from the plasma membrane. * $P < 0.05$; ** $P < 0.01$; *** $P < 0.001$.

PI3K γ regulates secretory granule recruitment to the plasma membrane. We further examined the role of p110 γ in insulin granule exocytosis by simultaneous TIRF and whole-cell capacitance measurements. In INS-1 833/15 cells expressing the granule marker VAMP-pHluorin, the capacitance response was abolished following p110 γ inhibition (40 nmol/l AS605240) (Fig. 3A and B). Similarly, the exocytotic event frequency measured by TIRF was reduced by 62% ($n = 7$, $P < 0.001$) following inhibition of p110 γ (Fig. 3C–E). Finally, after normalizing to the initial granule density, inhibition of p110 γ was no longer seen to blunt the exocytotic response (Fig. 3F), suggesting that the impaired exocytosis was likely not due to a reduced efficiency of Ca^{2+} -stimulated exocytosis, per se.

We therefore examined the effect of p110 γ knockdown on the density of membrane-associated insulin granules by targeting mCherry to secretory granules using neuropeptide Y (NPY) (29). TIRF microscopy revealed that knockdown of p110 γ results in a 38 and 41% reduction in membrane-associated secretory granules in INS-1 832/13 cells ($n = 15$ –16, $P < 0.001$) and human β -cells ($n = 29$ –30 cells from four donors, $P < 0.001$), respectively (Fig. 4A

and B). This was confirmed by electron microscopy in INS-1 832/13 cells (Fig. 4C and D), where inhibition of p110 γ (40 nmol/l AS605240) reduced the number of secretory granules near (<100 nm) the plasma membrane by 37% ($n = 55-56$, $P < 0.01$). Inhibition of p110 γ was also associated with an increased ($P < 0.05$) number of granules at >100 nm from the plasma membrane (Fig. 4D) and no change in overall granule density (not shown).

PI3K γ regulates cortical F-actin density. Since cortical actin network integrity is an important determining factor in secretory granule recruitment and docking (30–32), we studied the effect of p110 γ inhibition on cortical filamentous (F)-actin in INS-1 832/13 cells, human islets, and mouse β -cells. The cortical F-actin network in INS-1 832/13 cells, assessed by TIRF microscopy, was increased after inhibition of p110 γ (40 nmol/l AS605240) (Fig. 5A). This was associated with a 53% reduction in the density of NPY-mCherry-labeled granules at the plasma membrane ($n = 20$, $P < 0.01$). Western blotting for purified F- and total globular (G)-actin confirmed that F-actin, as a proportion of total actin, was increased by p110 γ inhibition in INS-1 832/13 cells ($n = 3$, $P < 0.05$) and human islets ($n = 3$ donors, $P < 0.05$) (Fig. 5B and C).

The PtdIns(3,4,5)P₃ phosphatase activity of PTEN antagonizes PI3K signaling. We therefore examined the effect of p110 γ inhibition (40 nmol/l AS605240) on F-actin in control mouse β -cells (RIP-cre⁺) and those lacking PTEN (RIP-cre⁺/PTEN^{fl/fl}) (8). Cortical F-actin was visualized by epifluorescence microscopy (Fig. 6A). Analysis by random line scans (Fig. 6A, bottom) demonstrated that peak F-actin staining was increased 1.7-fold ($P < 0.001$, $n = 10-11$) by p110 γ inhibition in control β -cells but not in β -cells lacking PTEN ($n = 10-11$) (Fig. 6).

Acute F-actin disruption restores vesicle docking and exocytosis following PI3K γ inhibition. Since the reduction in membrane-associated granules is associated with increased cortical F-actin, we examined whether disruption of F-actin could restore the membrane localization of secretory granules and exocytosis following p110 γ inhibition. Inhibition of p110 γ (40 nmol/l AS605240) increased F-actin staining by twofold ($n = 25-26$, $P < 0.001$) (Fig. 7A and B). This was associated with a 37% ($n = 25-26$, $P < 0.001$) reduction in membrane-associated secretory granules, labeled in this experiment with a granule-targeted IAPP-mCherry construct.

As cAMP inhibits actin polymerization through protein kinase A-dependent phosphorylation of monomeric actin (33) and an indirect inhibition of the Rho family of GTPases (rev. in 34,35), we examined whether increased cAMP could reduce F-actin density and rescue granule recruitment following p110 γ inhibition. Indeed, acute treatment with the cAMP-raising agent forskolin (5 μ mol/l, 10 min) reversed the effects of p110 γ inhibition on cortical F-actin ($n = 34$, $P < 0.001$) and membrane granule density ($n = 30$, $P < 0.001$) in the INS-1 832/13 cells (Fig. 7A and B).

Additionally, 10-min treatment with the actin depolymerizing agent latrunculin (10 μ mol/l) reduced actin staining in both control ($n = 28$, $P < 0.001$) and AS605240-treated ($n = 21$, $P < 0.001$) INS-1 832/13 cells (Fig. 7A and B). This acute depolymerization of F-actin increased the density of membrane-associated vesicles by 2.2-fold compared with p110 γ inhibition alone ($n = 16$, $P < 0.001$) (Fig. 7A and B). Thus, secretory granules remain present in the cell following p110 γ inhibition and can reach the plasma membrane upon disruption of the cortical actin barrier.

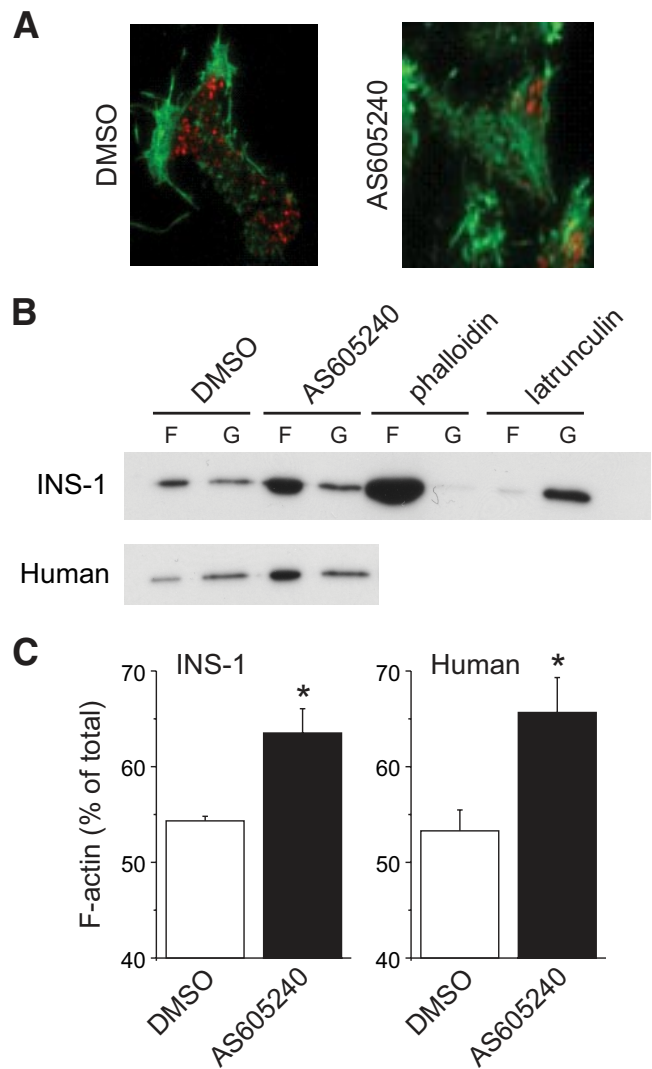


FIG. 5. Inhibition of p110 γ increases cortical F-actin. A: INS-1 832/13 cells expressing the granule targeted NPY-mCherry (red) were treated overnight with DMSO or AS605240 (40 nmol/l) and subsequently stained for F-actin with Alexa 488-conjugated phalloidin (green) and imaged by TIRF microscopy. B: The content of F-actin (F) and G-actin (G) was determined by immunoblotting of cell lysates from INS-1 832/13 cells and human islets treated overnight with DMSO or AS605240 (40 nmol/l). Acute (10 min) treatment with phalloidin (1 μ mol/l) or latrunculin (10 μ mol/l) were used as controls for actin polymerization and depolymerization, respectively. C: The F-actin content is shown as a percentage of total actin. * $P < 0.05$. (A high-quality digital representation of this figure is available in the online issue.)

Finally, acute forskolin treatment (5 μ mol/l, 10 min, $n = 25$) restored membrane-proximal granule density to control levels in INS-1 832/13 cells expressing si-p110 γ ($P < 0.05$) (Fig. 8A). Inclusion of cAMP (100 μ mol/l) in the patch-clamp pipette resulted in complete restoration of exocytosis following p110 γ knockdown ($n = 10$) (Fig. 8B and C). Similarly, the capacitance response of INS-1 832/13 (Fig. 8D and E) and human β -cells (Fig. 8F and G) to a single 500-ms depolarization from -70 to 0 mV, which was blunted in following p110 γ inhibition ($n = 14-20$, $P < 0.01$ and $n = 15-17$ cells from five donors, $P < 0.001$), could be rapidly reversed by intracellular dialysis of either 100 μ mol/l cAMP (INS-1, $n = 14$; human, $n = 9$ from five donors) or 10 μ mol/l latrunculin (INS-1, $n = 9$; human $n = 12$ from five donors). Thus, depolymerization of actin and

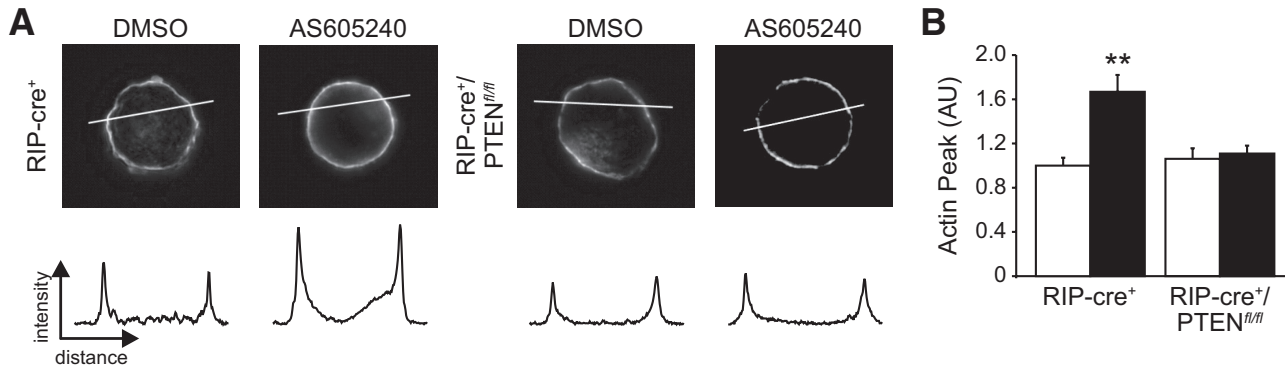


FIG. 6. The increase in cortical F-actin staining upon inhibition of p110 γ is prevented by deletion of PTEN. **A:** β -Cells from RIP-cre⁺ control mice or RIP-cre⁺/PTEN^{fl/fl} mice lacking the lipid phosphatase PTEN were stained for F-actin with Alexa Fluor 488-conjugated phalloidin and examined by epifluorescence. Representative images are shown at *top*, with intensity line scans for F-actin staining intensity *below*. **B:** The average F-actin peak intensities are shown. ** $P < 0.01$.

restoration of the membrane-associated granule pool is sufficient to rescue exocytosis following p110 γ inhibition.

DISCUSSION

Our previous work demonstrated that knockout of p110 γ results in a blunted glucose-stimulated insulin response, particularly during the first phase of secretion (18). We have now examined the underlying mechanism for regulation of insulin secretion by p110 γ . This PI3K isoform positively regulates the size of the membrane-associated pool of insulin granules, likely through the modulation of cortical F-actin density. Therefore, we now identify a previously undescribed role for PI3K γ in the regulation of cortical actin and targeting of insulin granules to the plasma membrane in pancreatic β -cells.

The tyrosine kinase-activated isoforms of PI3K (type 1A) account for as much as 80% of islet PI3K activity (3). The type 1B isoform, p110 γ , is expressed in insulinoma cells, rodent islets, and human islets (18) (Fig. 1), where it contributes a minor fraction of PI3K activity (17). The nonselective nature of commonly used PI3K inhibitors may account for earlier findings ascribing both negative (1–3) and positive (4,5) roles to PI3K in insulin secretion. Indeed, the various PI3Ks may play distinct roles in the regulation of insulin secretion in an isoform-specific manner. This is supported by the observation that while it displays basal activity (15), p110 γ is glucose-independent in INS-1 cells (17) and thus likely does not contribute to increased PI3K activity following autocrine insulin feedback (24). This is consistent with our finding that p110 γ inhibition did not blunt high K⁺-stimulated PtdIns(3,4,5)P₃ formation (see RESEARCH DESIGN AND METHODS).

Consistent with the lack of first-phase secretion in the p110 γ knockout mouse (18), we observed a reduction of the early exocytotic response during membrane depolarization in both INS-1 and human β -cells following p110 γ knockdown or pharmacological inhibition. This was paralleled by a similar reduction in the peak insulin secretory response to KCl following p110 γ inhibition in human islets. Reduced exocytosis was not due to the inhibition of voltage-dependent Ca²⁺ channel activity, and defective Ca²⁺ stimulated exocytosis was also demonstrated in response to direct Ca²⁺ infusion following knockdown of p110 γ . While the lack of exocytotic response to Ca²⁺ infusion during latter time points (i.e., 30–60 s) may be indicative of a reduced Ca²⁺-induced granule recruitment, since the readily releasable pool of granules is expected to

be already released (28), the exact role of p110 γ in glucose- and Ca²⁺-dependent granule recruitment, per se, remains unknown. Nonetheless, these results suggest a reduction in the size of the readily releasable granule pool and blunted refilling during prolonged Ca²⁺ stimulation.

There was no increase, and often a net negative change, in membrane capacitance in many experiments following p110 γ inhibition. This was most noticeable following pharmacological inhibition with AS605240, likely due to a more complete inhibition of p110 γ compared with the siRNA approach. The absence of a capacitance response is not necessarily indicative of an absence of exocytosis, however, since this reports the net balance of exocytosis and endocytosis. In the present context, since PtdIns(4,5)P₂ is an important regulator of endocytosis (36–38), a reduced capacitance response may result from an increased Ca²⁺-stimulated endocytosis (39). To address this, we simultaneously monitored exocytosis visually while measuring whole-cell capacitance changes in INS-1 cells. In these experiments, the exocytotic release of granule content was indeed blunted following p110 γ inhibition (Fig. 3).

Reduced exocytosis can be explained either by an inability of membrane-associated granules to undergo exocytosis in response to a Ca²⁺ stimulus or simply by a lack of membrane-associated granules. While impaired synaptic-like vesicle exocytosis may also contribute, the present data clearly demonstrate a reduced membrane-localized insulin granule pool by electron microscopy analysis, consistent with our TIRF imaging. This is not secondary to reduced insulin content since this is increased in the p110 γ knockout mice (18) and following p110 γ knockdown in INS-1 cells (18), whole-cell insulin staining is increased in mouse β -cells following p110 γ inhibition (not shown), and acute disruption of F-actin can rapidly recover insulin granules at the plasma membrane (Fig. 7).

The integrity of the cortical F-actin network is an important determinant of granule recruitment to the plasma membrane in chromaffin (30) and β -cells (31,32). The cortical actin network can act as a physical barrier to granule translocation (40) and can inhibit granule docking through the direct occlusion of syntaxin 4 binding sites (31). Indeed, decreased membrane-associated insulin granule density following p110 γ inhibition is associated with increased F-actin (Figs. 5–7). While we have not examined the time course of F-actin changes, we have observed that overnight inhibition of p110 γ is required to

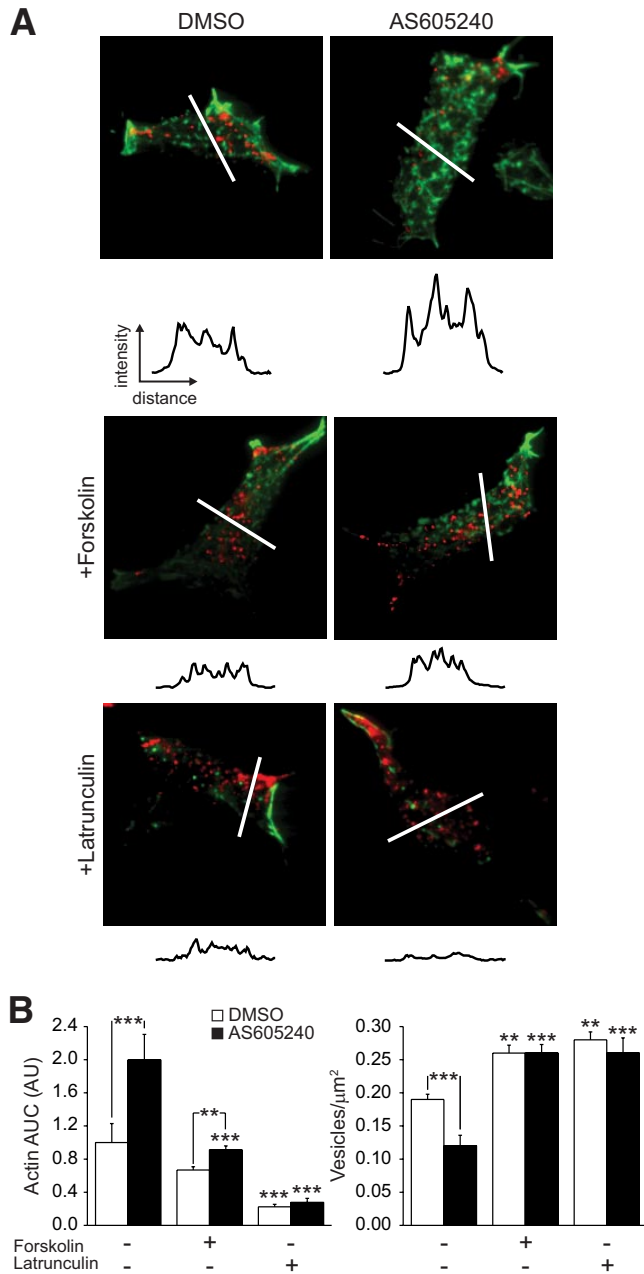


FIG. 7. Disruption of the F-actin network rescues membrane targeting of granules following p110 γ inhibition. **A:** INS-1 832/13 cells expressing the granule-targeted IAPP-mCherry construct (red) were treated overnight with DMSO or 40 nmol/l AS605240 then for 10 min with forskolin (5 $\mu\text{mol/l}$) or latrunculin (10 $\mu\text{mol/l}$), as indicated, and imaged by TIRF microscopy following staining for actin (green). Intensity line scans, obtained in a double-blinded manner, for actin from the regions indicated are shown. Average actin line-scan area under the curve and membrane-associated granule density are shown in **B**. ** $P < 0.01$; *** $P < 0.001$ vs. control, unless indicated otherwise. (A high-quality digital representation of this figure is available in the online issue.)

blunt the exocytotic response (not shown). We ascribe this to the time necessary for the depletion of the membrane-associated granule pool. Thus, the overall reduction of membrane-associated granules following p110 γ inhibition is likely related to the rate at which preexisting membrane-associated granules are either basally released or internally recycled. A functional role for increased F-actin density in the inhibition of granule trafficking to the plasma membrane is demonstrated by the ability of actin

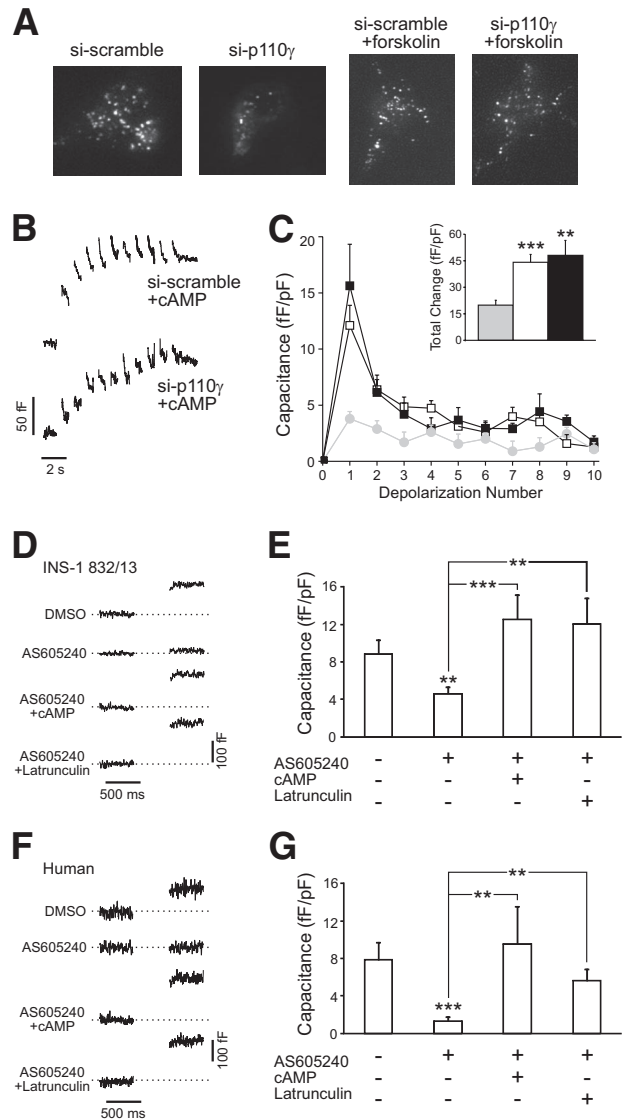


FIG. 8. Disruption of the F-actin network rescues exocytosis following p110 γ inhibition. **A:** Membrane-associated secretory granules were visualized by TIRF microscopy in INS-1 832/13 cells coexpressing an NPY-mCherry and either si-scramble or si-p110 γ . Addition of forskolin (5 $\mu\text{mol/l}$, 10 min) resulted in the recovery of membrane-associated secretory granules. **B:** Representative membrane capacitance traces are shown from INS-1 832/13 cells expressing si-scramble or si-p110 γ with 100 $\mu\text{mol/l}$ cAMP included in the patch pipette. **C:** The average capacitance response for each depolarization and the total response over the course of the depolarization train (*inset*) for cells expressing si-scramble (open symbols) or si-p110 γ (black symbols) with cAMP in the patch pipette. The response from cells expressing si-p110 γ in the absence of cAMP is also shown for comparison (gray symbols). **D:** Representative membrane capacitance responses to a single depolarization from -70 to 0 mV by INS-1 832/13 cells treated with DMSO or the p110 γ inhibitor alone or with 100 $\mu\text{mol/l}$ cAMP or 10 $\mu\text{mol/l}$ latrunculin in the patch pipette. **E:** Average capacitance responses. **F** and **G:** Shown the same as **D** and **E** but with human β -cells. ** $P < 0.01$; *** $P < 0.001$ vs. control, unless indicated otherwise.

depolymerization to acutely restore granule targeting and exocytosis (Fig. 7).

Only a minor fraction of the PI3K activity in insulin-secreting cells is contributed by p110 γ (17), making it difficult to determine the effect of p110 γ inhibition on whole-cell phosphoinositide levels. A role for p110 γ lipid kinase activity in the regulation of cortical F-actin density is, however, indicated by the ability of the ATP-competitive inhibitor AS605240 (23) to mimic the effect of p110 γ

knockdown and the reversal of this by deletion of the PtdIns(3,4,5)P₃ phosphatase PTEN. The exact mechanism by which p110 γ regulates cortical F-actin remains unclear, as phosphoinositides are complex regulators of cytoskeletal rearrangement (41,42). It is interesting to note that the Rho GTPases, such as Rac1 and Cdc42 that have important roles in insulin secretion (43), also regulate actin and are activated by the lipid products of PI3K (44–46). Additionally, increased PtdIns(4,5)P₂, which may be secondary to p110 γ inhibition, could lead to actin assembly through the dissociation of actin capping proteins (including gelsolin) and/or activation of the WASP family proteins and the Arp2/3 complex (47). Thus, several potential actin-regulating proteins may act downstream of p110 γ .

The p110 γ isoform exhibits significant basal lipid kinase activity (15), and our results here suggest an important role for this in β -cell function. While it is unlikely that p110 γ is a key mediator of dynamic actin remodelling in response to glucose since it is not activated upon glucose-stimulation (17), a role in stimulated granule translocation cannot be ruled out since this PI3K isoform can be activated by the incretin hormone GIP in INS-1 cells (17). Furthermore, insulin secretion from HIT-T15 cells stimulated by GIP and the related VIP and PACAP peptides can be significantly blunted by wortmannin independent of cAMP generation, per se (4,5), similar to what we have observed with forskolin and the direct infusion of cAMP.

In summary, we now demonstrate that the p110 γ isoform of PI3K is necessary for insulin granule recruitment to the plasma membrane and maintenance of a membrane-associated readily releasable pool of secretory granules in model cell lines and in humans. This is mediated at least in part through the regulation of cortical F-actin and represents a previously unknown function for a nonclassical PI3K in the control of pancreatic β -cell function.

ACKNOWLEDGMENTS

This work was funded by an operating grant (to P.E.M.) from the Canadian Diabetes Association (CDA) and infrastructure grants from the Canada Foundation for Innovation and the Alberta Heritage Foundation for Medical Research (AHFMR). G.P. was supported in part by the British Council Researcher Exchange Program. J.K. was supported by the Alberta Diabetes Institute Wirtenan Studentship. B.J.B. was supported by an AHFMR summer studentship. Y.W.W. was supported by a summer studentship as part of a National Science and Engineering Research Council Discovery Grant to P.E.M. P.E.M. is a CDA and AHFMR Scholar and holds the Canada Research Chair in Islet Biology.

T.R. is an employee of Merck Serono and is involved in biomedical research, much of which is focused on P13 kinase pathways. No other potential conflicts of interest relevant to this article were reported.

C. Newgard (Duke University) provided the INS1 832/13 and 833/15 cells, G. Miesenboeck (Oxford) provided VAMP-pHluorin, G. Rutter (Imperial College London) provided NPY-mRFP, R. Tsien (UC San Diego) provided mCherry, and B. Nürnberg (HHU Düsseldorf, Germany) provided GFP-GRP1_{PH}. The authors are indebted to Nancy Smith for excellent technical support, Dr. Ming Chen for assistance with electron microscopy studies, and Drs. Patricia Brubaker and Peter Light for critical reading of the manuscript prior to submission.

REFERENCES

- Hagiwara S, Sakurai T, Tashiro F, Hashimoto Y, Matsuda Y, Nonomura Y, Miyazaki J. An inhibitory role for phosphatidylinositol 3-kinase in insulin secretion from pancreatic B cell line MIN6. *Biochem Biophys Res Commun* 1995;214:51–59
- Zawalich WS, Tesz GJ, Zawalich KC. Inhibitors of phosphatidylinositol 3-kinase amplify insulin release from islets of lean but not obese mice. *J Endocrinol* 2002;174:247–258
- Eto K, Yamashita T, Tsubamoto Y, Terauchi Y, Hirose K, Kubota N, Yamashita S, Taka J, Satoh S, Sekihara H, Tobe K, Ino M, Noda M, Kimura S, Kadowaki T. Phosphatidylinositol 3-kinase suppresses glucose-stimulated insulin secretion by affecting post-cytosolic [Ca²⁺]_i elevation signals. *Diabetes* 2002;51:87–97
- Straub SG, Sharp GW. Glucose-dependent insulinotropic polypeptide stimulates insulin secretion via increased cyclic AMP and [Ca²⁺]_i and a wortmannin-sensitive signalling pathway. *Biochem Biophys Res Commun* 1996;224:369–374
- Straub SG, Sharp GW. A wortmannin-sensitive signal transduction pathway is involved in the stimulation of insulin release by vasoactive intestinal polypeptide and pituitary adenylate cyclase-activating polypeptide. *J Biol Chem* 1996;271:1660–1668
- Kulkarni RN, Bruning JC, Winnay JN, Postic C, Magnuson MA, Kahn CR. Tissue-specific knockout of the insulin receptor in pancreatic beta cells creates an insulin secretory defect similar to that in type 2 diabetes. *Cell* 1999;96:329–339
- Kulkarni RN, Holzenberger M, Shih DQ, Ozcan U, Stoffel M, Magnuson MA, Kahn CR. β -Cell-specific deletion of the Igf1 receptor leads to hyperinsulinemia and glucose intolerance but does not alter β -cell mass. *Nat Genet* 2002;31:111–115
- Kulkarni RN, Winnay JN, Daniels M, Bruning JC, Flier SN, Hanahan D, Kahn CR. Altered function of insulin receptor substrate-1-deficient mouse islets and cultured beta-cell lines. *J Clin Invest* 1999;104:R69–R75
- Nguyen KT, Tajmir P, Lin CH, Liadis N, Zhu XD, Eweida M, Tolasa-Karaman G, Cai F, Wang R, Kitamura T, Belsham DD, Wheeler MB, Suzuki A, Mak TW, Woo M. Essential role of Pten in body size determination and pancreatic beta-cell homeostasis in vivo. *Mol Cell Biol* 2006;26:4511–4518
- Stephens LR, Jackson TR, Hawkins PT. Agonist-stimulated synthesis of phosphatidylinositol(3,4,5)-trisphosphate: a new intracellular signalling system? *Biochimica et Biophysica Acta (BBA) Mol Cell Res* 1993;1179:27–75
- Aspinwall CA, Qian WJ, Roper MG, Kulkarni RN, Kahn CR, Kennedy RT: Roles of insulin receptor substrate-1, phosphatidylinositol 3-kinase, and release of intracellular Ca²⁺ stores in insulin-stimulated insulin secretion in β -cells. *J Biol Chem* 2000;275:22331–22338
- Chasserot-Golaz S, Hubert P, Thierse D, Dirrig S, Vlahos CJ, Aunis D, Bader MF. Possible involvement of phosphatidylinositol 3-kinase in regulated exocytosis: Studies in chromaffin cells with inhibitor LY294002. *J Neurochem* 1998;70:2347–2356
- Gatof D, Kilic G, Fitz JG. Vesicular exocytosis contributes to volume-sensitive ATP release in biliary cells. *Am J Physiol Gastrointest Liver Physiol* 2004;286:G538–G546
- Koyasu S. The role of PI3K in immune cells. *Nat Immunol* 2003;4:313–319
- Sasaki AT, Janetopoulos C, Lee S, Charest PG, Takeda K, Sundheimer LW, Meili R, Devreotes PN, Firtel RA. G protein-independent Ras/PI3K/F-actin circuit regulates basic cell motility. *J Cell Biol* 2007;178:185–191
- Ruckle T, Schwarz MK, Rommel C. PI3K γ inhibition: towards an 'aspirin of the 21st century'? *Nat Rev Drug Discov* 2006;5:903–918
- Trumper A, Trumper K, Trusheim H, Arnold R, Goke B, Horsch D. Glucose-dependent insulinotropic polypeptide is a growth factor for β (INS-1) cells by pleiotropic signaling. *Mol Endocrinol* 2001;15:1559–1570
- MacDonald PE, Joseph JW, Yau D, Diao J, Asghar Z, Dai F, Oudit GY, Patel MM, Backx PH, Wheeler MB. Impaired glucose-stimulated insulin secretion, enhanced IP insulin tolerance and increased β -cell mass in mice lacking the p110 γ isoform of PI3-kinase. *Endocrinology* 2004;145:4078–4083
- Li LX, MacDonald PE, Ahn DS, Oudit GY, Backx PH, Brubaker PL. Role of phosphatidylinositol 3-kinase- γ in the β -cell: interactions with glucagon-like peptide-1. *Endocrinology* 2006;147:3318–3325
- Chen G, Hohmeier HE, Gasa R, Tran W, Newgard CB. Selection of insulinoma cell lines with resistance to interleukin-1 β and γ -interferon-induced cytotoxicity. *Diabetes* 2000;49:562–770
- Hohmeier HE, Mulder H, Chen G, Henkel-Rieger R, Prentki M, Newgard CB. Isolation of INS-1-derived cell lines with robust ATP-sensitive K⁺ channel-dependent and independent glucose-stimulated insulin secretion. *Diabetes* 2000;49:424–430
- Obermuller S, Lindqvist A, Karanaukaite J, Galvanovskis J, Rorsman P,

- Barg S. Selective nucleotide-release from dense-core granules in insulin-secreting cells. *J Cell Sci* 2005;118:4271–4282
23. Camps M, Ruckle T, Ji H, Ardissone V, Rintelen F, Shaw J, Ferrandi C, Chabert C, Gillieron C, Francon B, Martin T, Gretener D, Perrin D, Leroy D, Vitte PA, Hirsch E, Wymann MP, Cirillo R, Schwarz MK, Rommel C. Blockade of PI3K γ suppresses joint inflammation and damage in mouse models of rheumatoid arthritis. *Nat Med* 2005;11:936–943
 24. Barker CJ, Leibiger IB, Leibiger B, Berggren PO. Phosphorylated inositol compounds in β -cell stimulus-response coupling. *Am J Physiol Endocrinol Metab* 2002;283:E1113–E1122
 25. Brock C, Schaefer M, Reusch HP, Czupalla C, Michalke M, Spicher K, Schultz G, Nurnberg B. Roles of G $\beta\gamma$ in membrane recruitment and activation of p110 γ /p101 phosphoinositide 3-kinase γ . *J Cell Biol* 2003;160:89–99
 26. Muller D, Huang GC, Amiel S, Jones PM, Persaud SJ. Gene expression heterogeneity in human islet endocrine cells in vitro: the insulin signalling cascade. *Diabetologia* 2007;50:1239–1242
 27. Guillermet-Guibert J, Bjorklof K, Salpekar A, Gonella C, Ramadani F, Bilancio A, Meek S, Smith AJ, Okkenhaug K, Vanhaesebroeck B. The p110 β isoform of phosphoinositide 3-kinase signals downstream of G protein-coupled receptors and is functionally redundant with p110 γ . *Proc Natl Acad Sci U S A* 2008;105:8292–8297
 28. Kanno T, Ma X, Barg S, Eliasson L, Galvanovskis J, Gopel S, Larsson M, Renstrom E, Rorsman P. Large dense-core vesicle exocytosis in pancreatic beta-cells monitored by capacitance measurements. *Methods* 2004;33:302–311
 29. Tsuboi T, Rutter GA. Multiple forms of “kiss-and-run” exocytosis revealed by evanescent wave microscopy. *Curr Biol* 2003;13:563–567
 30. Burgoyne RD, Cheek TR. Reorganisation of peripheral actin filaments as a prelude to exocytosis. *Biosci Rep* 1987;7:281–288
 31. Jewell JL, Luo W, Oh E, Wang Z, Thurmond DC. Filamentous actin regulates insulin exocytosis through direct interaction with Syntaxin 4. *J Biol Chem* 2008;283:10716–10726
 32. Li G, Rungger-Brandle E, Just I, Jonas JC, Aktories K, Wollheim CB. Effect of disruption of actin filaments by Clostridium botulinum C2 toxin on insulin secretion in HIT-T15 cells and pancreatic islets. *Mol Biol Cell* 1994;5:1199–1213
 33. Ohta Y, Akiyama T, Nishida E, Sakai H. Protein kinase C and cAMP-dependent protein kinase induce opposite effects on actin polymerizability. *FEBS Lett* 1987;222:305–310
 34. Howe AK. Regulation of actin-based cell migration by cAMP/PKA. *Biochim Biophys Acta* 2004;1692:159–174
 35. Roscioni SS, Elzinga CR, Schmidt M. Epac: effectors and biological functions. *Naunyn Schmiedebergs Arch Pharmacol* 2008;377:345–357
 36. Sun Y, Carroll S, Kaksonen M, Toshima JY, Drubin DG. PtdIns(4,5)P₂ turnover is required for multiple stages during clathrin- and actin-dependent endocytic internalization. *J Cell Biol* 2007;177:355–367
 37. Jost M, Simpson F, Kavran JM, Lemmon MA, Schmid SL. Phosphatidylinositol-4,5-bisphosphate is required for endocytic coated vesicle formation. *Curr Biol* 1998;8:1399–1402
 38. Zoncu R, Perera RM, Sebastian R, Nakatsu F, Chen H, Balla T, Ayala G, Toomre D, De Camilli PV. Loss of endocytic clathrin-coated pits upon acute depletion of phosphatidylinositol 4,5-bisphosphate. *Proc Natl Acad Sci U S A* 2007;104:3793–3798
 39. MacDonald PE, Eliasson L, Rorsman P. Calcium increases endocytotic vesicle size and accelerates membrane fission in insulin secreting INS-1 cells. *J Cell Sci* 2005;118:5911–5920
 40. Rutter GA, Hill EV. Insulin vesicle release: walk, kiss, pause: then run. *Physiology (Bethesda)* 2006;21:189–196
 41. Insall RH, Weiner OD. PIP₃, PIP₂, cell movement: similar messages, different meanings? *Dev Cell* 2001;1:743–747
 42. Tsakiridis T, Tong P, Matthews B, Tsiani E, Bilan PJ, Klip A, Downey GP. Role of the actin cytoskeleton in insulin action. *Microsc Res Tech* 1999; 47:79–92
 43. Yin HL, Janmey PA. Phosphoinositide regulation of the actin cytoskeleton. *Annu Rev Physiol* 2003;65:761–789
 44. Wang Z, Oh E, Thurmond DC. Glucose-stimulated Cdc42 signaling is essential for the second phase of insulin secretion. *J Biol Chem* 2007;282: 9536–9546
 45. Ridley AJ, Rho GT. Pases and actin dynamics in membrane protrusions and vesicle trafficking. *Trends Cell Biol* 2006;16:522–529
 46. Welch HC, Coadwell WJ, Stephens LR, Hawkins PT. Phosphoinositide 3-kinase-dependent activation of Rac. *FEBS Lett* 2003;546:93–97
 47. Schmidt A, Hall A. Guanine nucleotide exchange factors for Rho GTPases: turning on the switch. *Genes Dev* 2002;16:1587–1609